THE JOURNAL OF BIOLOGICAL CHEMISTRY VOL. 285, NO. 20, pp. 15627–15636, May 14, 2010

Dicalcin Inhibits Fertilization through Its Binding to a Glycoprotein in the Egg Envelope in *Xenopus laevis*[*] [S]

Received for publication, November 5, 2009, and in revised form, March 15, 2010 Published, JBC Papers in Press, March 18, 2010, DOI 10.1074/jbc.M109.079483

Naofumi Miwa[‡1], **Motoyuki Ogawa**[§], **Yukiko Shinmyo**[¶], **Yoshiki Hiraoka**[‖], **Ken Takamatsu**[‡], **and Satoru Kawamura**[¶]

From the [‡]*Department of Physiology, School of Medicine, Toho University, 5-21-16 Ohmori-nishi, Ohta-ku, Tokyo 143-8540, the* [§]*Department of Medical Education, School of Medicine, Kitasato University, 1-15-1 Kitasato, Sagamihara, Kanagawa 228-8555, the* [¶]*Graduate School of Frontier Biosciences, Osaka University, Yamada-oka 1-3, Suita, Osaka 565-0871, and the* [‖]*Department of Anatomy, School of Medicine, Keio University, 15 Shinano-machi, Shinjyuku-ku, Tokyo 160-0016, Japan*

Fertilization comprises oligosaccharide-mediated sperm-egg interactions, including sperm binding to an extracellular egg envelope, sperm penetration through the envelope, and fusion with an egg plasma membrane. We show that *Xenopus* dicalcin, an S100-like Ca^{2+}-binding protein, present in the extracellular egg envelope (vitelline envelope (VE)), is a suppressive mediator of sperm-egg interaction. Preincubation with specific antibody greatly increased the efficiency of *in vitro* fertilization, whereas prior application of exogenous dicalcin substantially inhibited fertilization as well as sperm binding to an egg and *in vitro* sperm penetration through the VE protein layer. Dicalcin showed binding to protein cores of gp41 and gp37, constituents of VE, in a Ca^{2+}-dependent manner and increased *in vivo* reactivity of VE with a lectin, *Ricinus communis* agglutinin I, which was accounted for by increased binding ability of gp41 to the lectin and greater exposure of gp41 to an external environment. Our findings strongly suggest that dicalcin regulates the distribution of oligosaccharides within the VE through its binding to the protein core of gp41, probably by modulating configuration of oligosaccharides on gp41 and the three-dimensional structure of VE framework, and thereby plays a pivotal role in sperm-egg interactions during fertilization.

Fertilization is an essential process whereby individual gametes unite to develop a new organism. This enigmatic process requires the direct interaction between sperm and the egg extracellular envelope (1–3). This extracellular envelope of egg (called zona pellucida in mammals or vitelline envelope (VE)[2] in amphibians) contains several glycoproteins (called ZP proteins) that are conserved, to some extent, among a variety of animals (4). Considerable lines of evidence have indicated that oligosaccharides of these glycoproteins play a critical role in sperm-egg interaction. In a current model, one or more sperm surface proteins recognize oligosaccharides of glycoproteins in the egg envelope, and thereby, sperm undergoes acrosome reaction, penetrates the egg envelope, and fuses with an egg plasma membrane (5), and several potential components for the binding of sperm to egg envelope have been demonstrated (6, 7). In *Xenopus laevis*, VE is known to be composed of at least four ZP proteins (gp120, gp69/64, gp41, and gp37). Most sperm binding activity (~70%) has been attributed to *N*-linked oligosaccharides on gp41, and the rest to *N*-linked oligosaccharides on gp64 (8). The primary structure of gp41 contains two *N*-linked glycosylation sites (Asn^{82} and Asn^{113}), both of which are located within ZP domain (residues 13–274) (9, 10). Based on mass spectrometry analyses using enzyme-digested peptides, some structures of *N*-linked VE oligosaccharides are proposed (11). However, it remains elusive how oligosaccharides of gp41 function to establish proper sperm-egg interactions. We have recently cloned *Xenopus* dicalcin, an S100-like calcium-binding protein, in *Xenopus* eggs (12). S100 proteins form a family of small (10–14 kDa) calcium-binding proteins that regulate various extra- and intracellular activities (13, 14). The primary structure of dicalcin consists of two S100-like regions connected by a linker region, which features this protein as a "dimer form of S100 calcium-binding protein." Dicalcin was originally identified in frog (*Rana catesbeiana*) olfactory cilia as an intracellularly expressed Ca^{2+}-binding protein (15). The Ca^{2+}-bound form of dicalcin interacts with several ciliary proteins, including annexins and β-adrenergic receptor kinase-like protein (16, 17). Dicalcin shows no enzymatic activities by itself, and instead, through interactions with these intracellular target proteins, it may serve to regulate ciliary function(s) of olfactory neurons such as chemosensory signaling and/or ciliary membrane repair. After the original identification, however, this protein was also found in other tissues, including egg (12). The objectives of this study were to examine whether dicalcin regulates some reproductive functions, including fertilization and to identify molecular mechanisms for the action of dicalcin. We here characterized *Xenopus* dicalcin in egg and revealed its crucial role in sperm-egg interaction during fertilization.

EXPERIMENTAL PROCEDURES

Expression of Dicalcin in Escherichia coli—The coding region of dicalcin was PCR-amplified, ligated with pET-3a (Novagen, EMD, Darmstadt, Germany) and subsequently introduced into

* This work was supported by grants from the Japan Society for the Promotion of Science (to N. M. and S. K.) and by the Project Research of Toho University School of Medicine (to N. M.).

[S] The on-line version of this article (available at http://www.jbc.org) contains supplemental Fig. S1.

[1] To whom correspondence should be addressed. Tel.: 81-3-3762-4151; Fax: 81-3-3762-8225; E-mail: nmiwa@med.toho-u.ac.jp.

[2] The abbreviations used are: VE, vitelline envelope; PVDF, polyvinylidene difluoride; TFMS, trifluoromethanesulfonic acid; BSA, bovine serum albumin; TMR, tetramethylcarboxyrhodamine; FCS, fluorescent correlation spectroscopy; RCAI, *R. communis* agglutinin I; CBB, Coomassie brilliant blue.

E. coli BL21 pLysS (Novagen). Recombinant dicalcin was expressed and purified according to procedures as described previously (15).

^{45}Ca Blot Analysis—^{45}Ca blot analysis was performed as described previously (16). Recombinant dicalcin and molecular size markers (Bio-Rad, ~6 μg each) were electrophoresed and transferred onto a PVDF membrane (Immobilon, Millipore, Billerica, MA). Blots on the membrane were soaked in a Tris-buffered saline (100 mM Tris-HCl, 154 mM NaCl, pH 7.5) under 1 mM $^{45}CaCl_2$ (5.9×10^{12} Bq/mmol). After blots were washed with 50% methanol and then dried, bound ^{45}Ca was detected with BAS2000 (Fujifilm, Tokyo, Japan).

Ca^{2+} Binding Studies—To measure the stoichiometry of Ca^{2+} binding to dicalcin, we performed flow dialysis experiments as previously described (18). Briefly, we incubated dicalcin (final concentration, 10 μM) in a Tris buffer (100 mM KCl and 20 mM Tris-HCl, pH 7.5) at 20 °C with various concentrations of $^{45}CaCl_2$ (5.9×10^{12} Bq/mmol). The reaction buffer was placed in a prewashed microconcentrator (Microcon, Millipore) used as a filtration device, and then it was centrifuged briefly. We counted the activities of ^{45}Ca in 4-μl portions of both reaction mixture and the filtrate using a scintillation mixture (Clearzol, Nacalai, Kyoto, Japan). By comparing the activities of ^{45}Ca in the reaction mixture and the filtrate, the amount of Ca^{2+} bound to dicalcin was calculated. Blank experiments without dicalcin were performed to correct for nonspecific binding of Ca^{2+} to the membrane of microconcentrators. The Ca^{2+} concentration in each reaction mixture was varied using a Ca/EGTA buffering system and was calibrated fluorometrically with fluo-3 FF (19) (Calbiochem, EMD).

Western Blot Analysis—A soluble fraction of eggs was obtained by ultracentrifugation (50,000 × *g*, 30 min, 4 °C) of the egg homogenate. A portion of the soluble fraction was electrophoresed and transferred to a PVDF membrane (Immobilon P, Millipore). After blocking, blots were incubated with dicalcin antibody at 4 °C at a dilution of $1/(2 \times 10^4)$. Anti-dicalcin antibody against purified recombinant dicalcin was raised in a rabbit. After washing, blots were reacted with a horseradish peroxidase-labeled secondary antibody. Immunoreactive proteins were visualized by LAS-1000 (Fujifilm).

Affinity Purification of Anti-dicalcin Antibody—Anti-dicalcin antibody was immunoaffinity-isolated from an antiserum using dicalcin-Sepharose. Preparation of dicalcin-Sepharose was performed as described previously (16).

Immunohistochemistry—A *Xenopus* egg was first dejellied by using 2% cysteine and fixed in 2% paraformaldehyde, 0.2% glutaraldehyde, and 0.1% Triton at 4 °C. Then the egg was immersed in 25% sucrose, embedded in O.C.T. compound (Tissue-Tek, Sakura Finetek, Tokyo, Japan), and cut into ~14-μm-thick sections. The sections were then treated by a standard immunohistochemical procedures in which anti-dicalcin antibody was used at a dilution of $1/(2 \times 10^4)$ at 4 °C overnight. After the sections were rinsed, they were treated with a secondary antibody (Alexa 568, Molecular Probes, Invitrogen).

VE Protein Preparation—VE proteins were prepared from *Xenopus* eggs by sieving method described elsewhere (20, 21). Briefly, envelopes were collected by passing dejellied egg lysate through a nylon screen, and the screen was washed extensively with distilled water. Isolated envelopes were stored overnight in 2 M NaCl, 2 mM $CaCl_2$, 10 mM Tris-HCl (pH 7.4) to selectively solubilize contaminating yolk platelets (22), and heated at 70 °C before use.

Chemical Deglycosylation of VE Proteins—VE proteins were deglycosylated using trifluoromethanesulfonic acid (TFMS) as described elsewhere (23). Briefly, freeze-dried VE proteins were suspended in 100 μl of anhydrous TFMS/anisole (9:1) and kept on ice during 3 h. After this cleavage reaction, 1 ml of pyridine/diethylether (1:9) was added to the reaction mixture in a dry ice/ethanol bath to remove TFMS. Deglycosylated VE proteins were dialyzed against 10 mM NH_4HCO_3.

Blot Overlay Analysis—Blot overlay analysis using biotinylated dicalcin was performed according to our previous method (16). Soluble egg proteins and VE were electrophoresed and blotted onto a PVDF membrane. Deglycosylated VE proteins were used when indicated. After renaturing and blocking, blots were incubated with biotinylated dicalcin (final concentration, 0.4 μM) overnight at 4 °C in the presence of either 500 μM $CaCl_2$ or 500 μM EGTA. When blots were incubated with Rhodamine-labeled *Ricinus communis* agglutinin I (RCAI), they were preincubated with dicalcin in the presence of either $CaCl_2$ or EGTA. After wash, biotinylated dicalcin bound to a target protein was coupled to horseradish peroxidase using a Vectastain ABC kit (Vector Laboratories, Burlingame, CA) and visualized by using LAS-1000 (Fujifilm). Bound Rhodamine-labeled RCAI was visualized by using FLA-8000 (Fujifilm).

Preparation of Gametes—Ovulated or gently squeezed eggs were immediately washed three times with Steinberg solution (58 mM NaCl, 0.6 mM KCl, 0.3 mM $Ca(NO_3)_2$, 0.8 mM $MgSO_4$, 5 mM Tris, pH 7.4). Jelly was removed by exposure (5 min) of the eggs to 2% cysteine. The resultant jelly-free eggs were gently washed several times with 0.3×MMR (1×MMR: 100 mM NaCl, 2 mM KCl, 1 mM $MgCl_2$, 2 mM $CaCl_2$, 0.1 mM EDTA, 5 mM Hepes, pH 7.8). Jelly extract was prepared as described elsewhere (24). Briefly, jelly-coated eggs (~4g) were subjected to gentle rocking with 10 ml of 0.3×MMR for 60 min. The medium was collected and mixed with Ficoll (final concentration, 10%, Sigma), providing "jelly extract." Sperm were prepared by chopping and macerating a freshly excised testis in 1 ml of 0.3×MMR. The intact sperm were diluted in the jelly extract.

Sperm Binding Assay—Approximately 40 dejellied eggs in 0.3×MMR of ~500 μl were preincubated with the following material for 15 min; dicalcin (final concentration, 0.4 μM or 4 μM), BSA (4 μM) as a control, anti-dicalcin antibody (5 or 50 mg/liter), preimmune rabbit IgG (50 mg/liter). After washing eggs gently with 0.3×MMR, sperm suspension of ~100 μl (final concentration, $\sim 5 \times 10^6$/ml) was added, and the mixture was incubated for 15 min. Then, sperm-treated eggs were gently washed several times with 0.3×MMR. To confirm efficient removal of loosely attached sperm, two-cell embryos were treated in a same manner as controls. Almost no sperm (0–5 sperm/egg) remained attached to the two-cell embryo. The gametes were fixed and stained in 3% paraformaldehyde in

0.3×MMR, and bound sperm were counted in an equatorial focal plane. All count was done blind to conditions. For a quantitative confocal study, the gametes were fixed and stained in 3% paraformaldehyde in 0.3×MMR containing Hoechst 33342 (0.2 mg/ml). Stained sperm were observed using a confocal microscope (Zeiss LSM510, Oberkochen, Germany) with pinhole aperture, detector gain, and offset being kept constant for experimental comparisons. Intensity of Hoechst staining of each focal plane was summed from three stepwise focal planes having a 50-μm interval to score the total number of bound sperm per egg. All quantifications were done blind to conditions.

In Vitro Penetration Assay—We used Netwell assembly to assay the efficiency of sperm penetration (Netwell^{TM}, Corning, NY). The upper chamber is assembled from the polystyrene frame insert and the polyester mesh, the mesh size (~70 μm) of which is proper enough to hold viscous VE proteins and also to allow sperm for free moving. In the lower chamber, 650 μl of 0.3×MMR was filled to contact with the bottom mesh of the upper chamber. Suspension of VE proteins (0.5 mg/ml, ~650 μl) was placed on the mesh of the upper chamber. After preincubation of VE protein layer either with dicalcin (final concentration, 4 μM) or BSA (4 μM) as a control for 15 min, sperm suspension (~5 × 10^6 sperm/well) was added, and the mixture was incubated for the indicated time. Penetrated sperm through the VE to the lower chamber were collected and counted to calculate the percentage of penetrated sperm. All counts were done blind to conditions.

In Vitro Fertilization Assay—Pretreatments were performed similarly as described for the sperm binding assay. After washing gently with 0.3×MMR, dejellied eggs were inseminated with sperm (final concentration, ~5 × 10^6/ml) treated with jelly extract. The successful fertilization was scored by counting eggs that underwent first cleavage until some of the fertilized eggs proceeded to the four-cell stage (mostly occurring within ~120 min after insemination). All counts were done blind to conditions.

Lectin Blot Analyses and Lectin Cytochemistry—Lectin blot analyses were performed as described elsewhere (25). VE proteins were electrophoresed and blotted onto a PVDF membrane. Deglycosylated VE proteins were used where indicated. After blocking with synthetic polymer (PVDF Blocking Reagent, TOYOBO, Osaka, Japan), blots were probed with 50 μg/ml lectin conjugates (Rhodamine-RCAI, Fluorescein-soybean agglutinin, Fluorescein-*Sambucus nigra* lectin, and Biotinylated-MALII, Vector Laboratories). After wash, bound lectin was visualized by using FLA-8000 (Fujifilm) or LAS-1000 using a Vectastain ABC kit similarly as in blot overlay analysis. For lectin cytochemistry, unfertilized eggs were pretreated either with BSA or dicalcin (4 μM each) in 0.3×MMR at room temperature for 15 min. After wash, eggs were treated with Rhodamine-labeled RCAI (50 μg/ml) for 30 min and analyzed using a confocal microscope initially under low detector gain, followed by observation under high detector gain for further analyses.

Isolation and Fluorescent Labeling of gp41— gp41 was isolated under continuously eluted SDS-PAGE using a Mini Prep Cell (Bio-Rad) as previously described elsewhere (8). Briefly, heat-solubilized VE proteins were loaded onto a PAGE gel, and run with a constant current. Fractions were collected every 10 min with a flow rate of 60 μl/min. Fractions containing gp41 were analyzed by silver staining and pooled. Isolated gp41 was labeled with a fluorescent dye, tetramethylcarboxyrhodamine (TMR) according to the manufacturer's manual (protein labeling kit for the MF20 system, Olympus, Tokyo, Japan) and dialyzed against Tris-buffered saline.

FCS Analysis—Fluorescent correlation spectroscopy (FCS) measurements were performed in ~35 μl of a Tris-buffered saline (100 mM Tris-HCl, 154 mM NaCl, pH 7.5) solution containing TMR-labeled gp41 (10 nM), 200 μM Ca^{2+} either in the presence (1 μM) or absence of dicalcin (MF20 system, Olympus). Fluorescence intensity was recorded for the duration of 30 s at each measurement with a proper set of excitation light and emission filter, and diffusion time of each sample was calculated five times and averaged.

In Vivo VE Labeling with Cy5—Dejellied eggs were resuspended in 0.3×MMR (~500 μl) and labeled with 1 μl of Cy5 (final concentration, 1 nmol/ml; diluted from DIGE Fluor minimal dye of the Ettan DIGE system, Amersham Biosciences) on ice for 30 min. After quenching with 10 mM lysine, eggs were washed and VE proteins were isolated as described before. VE proteins were electrophoresed, and a fluorescence image was obtained using the fluorescence scanner (Typhoon 9400, Amersham Biosciences), followed by CBB staining to quantitate the amount of each VE protein. Based on fluorescence intensity, the molar amount of Cy5 coupled with VE protein was scored. Because one molecule of this dye couples with one molecule of protein (manufacturer's manual), we deduced the molar amount of labeled protein and calculated the ratio to total molar amount existing in the preparation for each of four VE proteins. Although the recommended pH for coupling buffer was 8.5 due to labeling efficiency of *N*-hydroxysuccinimide ester coupling chemistry, our coupling buffer with a pH of 7.5 was found to be also applicable to label VE proteins (supplemental Fig. S1), and therefore we adopted the pH of 7.5 for coupling in our assay as a more physiological condition.

Animal Care—All animal experiments were approved and in accordance with the animal care committee's guidelines at Toho University.

Statistical Analyses—Data are presented as mean ± S.E. otherwise indicated. The variables between two groups were analyzed using the Student *t* test.

RESULTS

Ca^{2+} Binding Activity of Xenopus Dicalcin—We first examined the protein chemistry of dicalcin for Ca^{2+} binding (Fig. 1). Our ^{45}Ca blot and flow dialysis experiments showed that dicalcin actually binds to approximately four Ca^{2+} per molecule maximally (~3.6 Ca^{2+}/protein at ~200 μM Ca^{2+} (Fig. 1*B*)). This indicates that all four Ca^{2+}-binding motifs called EF-hands are capable of interacting with Ca^{2+} and implies a potency of Ca^{2+}-dependent function(s) of dicalcin.

Localization of Dicalcin in Xenopus Egg—By using specific antibody against dicalcin (Fig. 2*A*), we examined localization

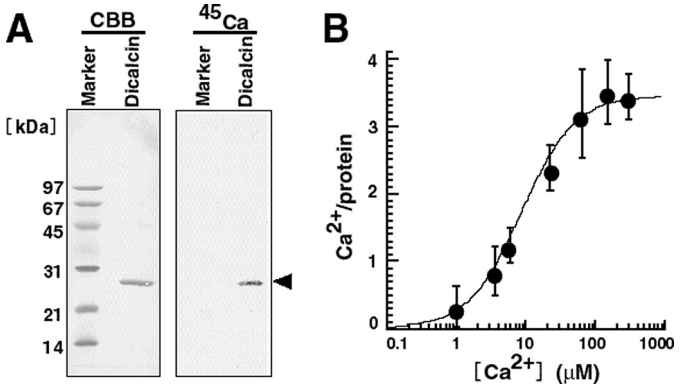

FIGURE 1. **Ca^{2+} binding activity of *Xenopus* dicalcin.** *A*, ^{45}Ca blot of *Xenopus* dicalcin. Recombinant dicalcin and molecular size markers (~6 μg each) were electrophoresed and transferred onto a PVDF membrane. Blots of recombinant *Xenopus* dicalcin and size markers were soaked in Tris-buffered saline containing 1 mM $^{45}CaCl_2$. After washing, the membrane was dried, and bound ^{45}Ca was detected. *CBB*, Coomassie brilliant blue staining; *^{45}Ca*, ^{45}Ca blot; *Marker*, molecular size markers; *Dicalcin*, recombinant *Xenopus* dicalcin. *B*, Ca^{2+} binding to *Xenopus* dicalcin. Recombinant dicalcin (final concentration, 10 μM) was incubated with various concentrations of $^{45}CaCl_2$. The *graph* shows the amount of Ca^{2+} bound to *Xenopus* dicalcin as a function of free Ca^{2+} concentration ($n = 6$, mean ± S.D.). The data were fitted by a Hill equation (*solid line*).

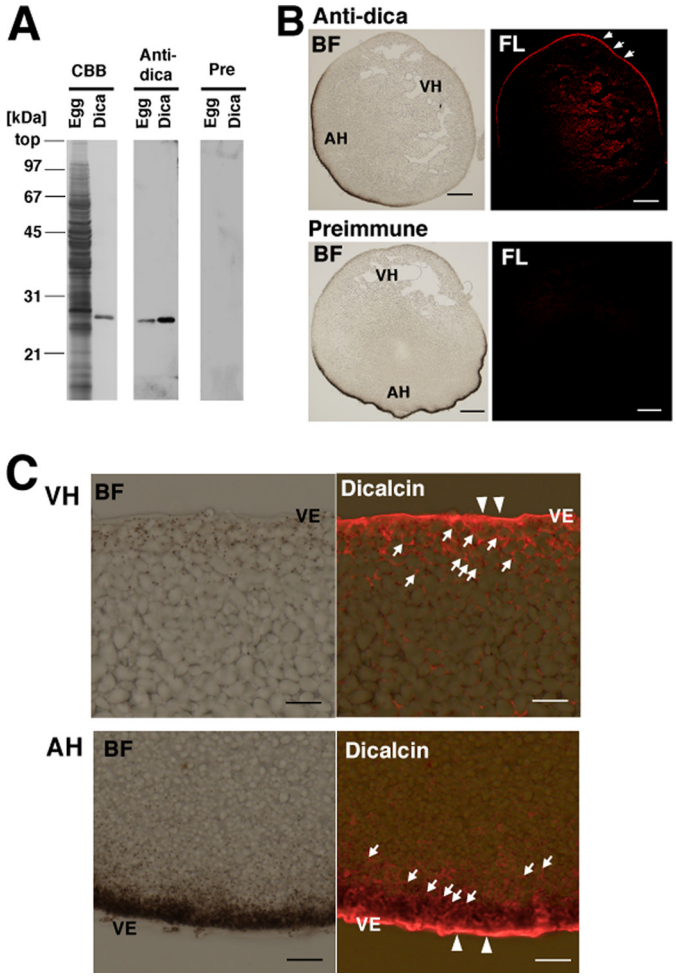

FIGURE 2. **Localization of dicalcin in *Xenopus* eggs.** *A*, specificity of anti-dicalcin antibody. *Left* (*CBB*): CBB staining of the proteins after SDS-PAGE of the homogenate of *Xenopus* eggs (*Egg*) and recombinant dicalcin (*Dica*). *Middle* (*Anti-dica*): Western blot analysis of homogenates of *Xenopus* eggs (*Egg*) and recombinant dicalcin (*Dica*) treated with anti-dicalcin antibody. *Right* (*Pre*): Blots treated with preimmune antibody. *B*, immunohistochemical staining at a low magnification. Eggs were fixed, and serial sections (~14-μm thickness) were treated with anti-dicalcin antibody (*Anti-dica*) or preimmune antibody (*Preimmune*). Dicalcin is localized in the marginal area of *Xenopus* eggs (arrows). *BF*, bright field observation; *FL*, fluorescence image. *Anti-dica*, stained with anti-dicalcin antibody; *Preimmune*, stained with preimmune antibody. *Scale bar*: 200 μm. *C*, detailed localization of dicalcin in *Xenopus* eggs. Dicalcin is localized in the extracellular vitelline envelope (*arrowheads*) and in the cytosolic cortex of the egg (*arrows*). *BF*, bright field observation; *Dicalcin*, merged image of bright field and fluorescence image stained with anti-dicalcin antibody. *VH*, vegetal hemisphere; *AH*, animal hemisphere; and *VE*, vitelline envelope. *Scale bar*: 20 μm.

of dicalcin in a *Xenopus* egg. The result showed that dicalcin is localized prominently in the marginal region of an egg and throughout the egg to a less extent (Fig. 2*B*). Higher magnified observation revealed that dicalcin is distributed uniformly in the VE (Fig. 2*C*, *arrowheads*). This result is intriguing, because no other S100 proteins have been shown to exist in the extracellular structure such as VE, although several lines of evidence demonstrated extracellular release of some S100 proteins (26, 27). In addition, dicalcin is localized in the cytosol within ~20 μm of depth from the cell surface: this area corresponds to the cortex of an egg (Fig. 2*C*, *arrows*), but not in yolk nor pigment granules. The absence of dicalcin within cortical granules suggests that extracellular release of dicalcin after fertilization is unlikely, consistent with our results that there were no significant changes in immunoreactive intensity between unfertilized and fertilized eggs (data not shown).

Ca^{2+}-dependent Binding of Dicalcin to Protein Cores of gp41 and gp37—To investigate the physiological role(s) of dicalcin in an egg, we tried to identify the target(s) of dicalcin. Blots of egg-soluble proteins and VE proteins were probed by biotinylated dicalcin either in the presence or absence of Ca^{2+}. Dicalcin bound to several egg and VE proteins in the presence of Ca^{2+} (*middle panels* in Fig. 3*A*, *arrowheads*), but not in the absence of Ca^{2+} (*right panels* in Fig. 3*A*). In egg extract, two bands at molecular masses of ~35–38 kDa may represent annexins that have been shown to interact with dicalcin in frog olfactory and respiratory cilia (17). VE is known to be composed of four major proteins (gp120, gp69/64, gp41, and gp37; *asterisks* in the *left panels* in Fig. 3*A*). A comparison of the molecular masses of the candidates (*arrowheads*) and silver-stained proteins (*asterisks*) revealed that dicalcin-binding proteins in the VE are gp41 and gp37. Dicalcin binding to gp41 or gp37 is specific, because dicalcin-binding signals almost disappeared in the presence of purified anti-dicalcin antibody (50 mg/liter) (Fig. 3*B*). It should be noted that this result also endorses the potential use of this polyclonal antibody to inhibit the interaction between dicalcin and VE proteins in the later *in vitro* fertilization experiment. Because gp41 and gp37 contain sugar moieties on their protein cores, we examined whether dicalcin binds to their protein cores or glycan portions. VE proteins were chemically deglycosylated using TFMS (*right lane* in Fig. 3*C*). TFMS-treated gp41 and gp37 co-migrated on SDS-PAGE at ~36 kDa as seen in previous research (23) (*upper panel*, Fig. 3*C*). The decrease in the apparent molecular mass after deglycosylation was larger in gp41 than in gp37, which is consistent with the notion that gp41 has as much as ~70% of total glycans in the VE glycoproteins (11). Our lectin blot showed that RCAI

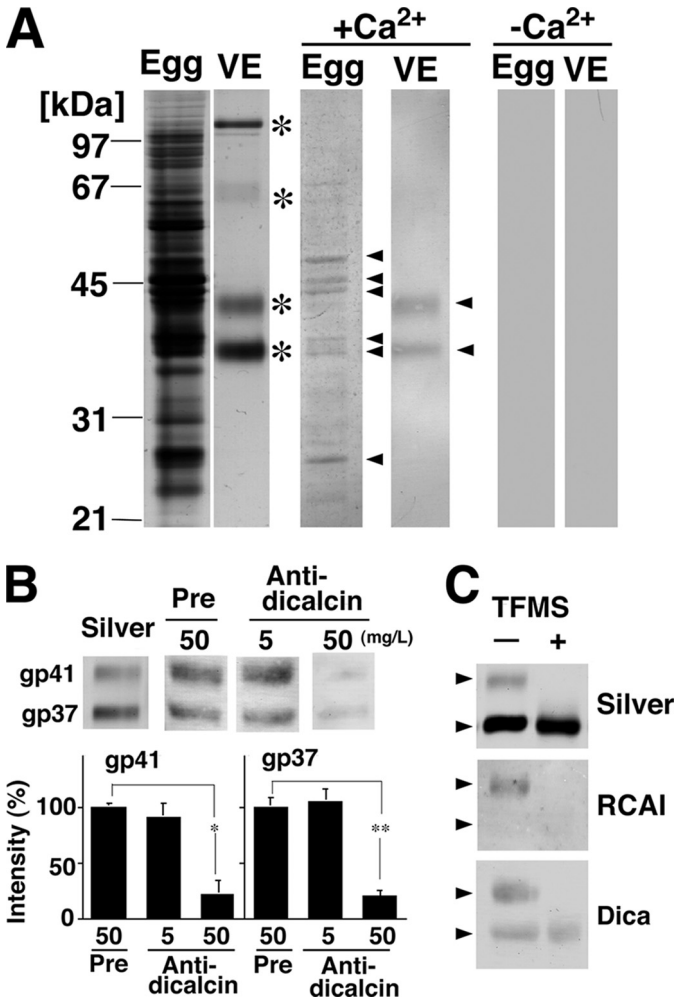

FIGURE 3. **Ca^{2+}-dependent binding of dicalcin to protein cores of gp41 and gp37.** *A*, dicalcin binds to several egg and VE proteins. Soluble egg proteins and vitelline envelope (*VE*) proteins were prepared as stated under "Experimental Procedures." VE proteins are composed of four major proteins (*asterisks*). Blots of both egg-soluble proteins and VE proteins were probed by biotinylated dicalcin either in the presence or absence of Ca^{2+}. Dicalcin bound to several egg proteins and two VE proteins (gp41 and gp37) in the presence of Ca^{2+} (*arrowheads*), but not in the absence of Ca^{2+}. *Egg*, soluble egg proteins; *VE*, VE proteins. $+Ca^{2+}$, blot overlay analysis in the presence of Ca^{2+} (500 μM $CaCl_2$); $-Ca^{2+}$, analysis in the absence of Ca^{2+} (500 μM EGTA). *B*, anti-dicalcin antibody inhibits the binding of dicalcin to gp41 and gp37. Blots of VE proteins were probed with biotinylated dicalcin either in the presence of anti-dicalcin antibody (*Anti-dicalcin*; 5 and 50 mg/liter) or preimmune antibody (*Pre*; 50 mg/liter). *Silver*, silver-stained VE proteins after SDS-PAGE; *Pre*, blot overlay analysis treated with preimmune antibody; *Anti-dicalcin*, blot overlay analysis treated with anti-dicalcin antibody. The *graph* shows mean data ($n = 6$; *, $p = 0.0015$; **, $p = 2.4 \times 10^{-5}$). *C*, dicalcin binds to deglycosylated forms of gp41 and gp37. VE proteins were treated with TFMS for 3 h. Blots of glycosylated and deglycosylated proteins were probed either with fluorescently labeled RCAI or biotinylated dicalcin. *Silver*, silver-stained proteins treated with TFMS (*TFMS* +) or without treatment (*TFMS* −); *RCAI*, blot with RCAI; *Dica*, blot with biotinylated dicalcin. *Arrowheads* indicate the positions of gp41 and gp37.

reacted solely with native gp41 but not with its TFMS-treated, deglycosylated form nor gp37 (*middle panel*, Fig. 3*C*). Our blot overlay analysis using deglycosylated VE proteins showed that dicalcin bound to ~36-kDa proteins (*lower panel*, Fig. 3*C*). Accordingly, these results indicate that dicalcin is likely to bind to protein cores of gp41 and gp37.

Inhibitory Effect of Dicalcin on Fertilization Processes—In a currently favored model of *Xenopus* sperm-egg interaction, acrosome-intact sperm bind to gp41 and gp69/64 and undergo acrosome reaction, which enables sperm to penetrate the VE (28). Major sperm binding activity has been shown to reside in the complex *N*-linked oligosaccharides of gp41 (8). In addition, a combination of gp37, gp41, and gp69/64 as a whole is suggested to maximize sperm binding, implying that gp37 serves to reinforce sperm binding to VE as an essential structural component of VE filaments (8). Because dicalcin binds to both gp37 and gp41 in the VE, we hypothesized that dicalcin affects the processes of sperm-egg interaction such as sperm binding to the VE and/or sperm penetration through the VE. To examine this, we first investigated the sperm-egg binding *in vitro* after preincubation of dejellied eggs either with BSA or anti-dicalcin antibody (50 mg/liter). The antibody slightly increased the number of bound sperm, although the extent is small (~115% of control, $n = 9$, $p = 0.027$) (Fig. 4*B*). In contrast, preincubation with recombinant dicalcin decreased the number of bound sperm (~77% of control at 4 μM, $n = 9$, $p = 0.003$) (Fig. 4*C*). In parallel, these findings were confirmed by confocal observations of the intensity of Hoechst-stained sperm bound to an egg (data not shown).

Next, to evaluate the effect of dicalcin on penetration through the VE, we developed an *in vitro* penetration assay method, where sperm were placed on a VE protein layer lying on a polycarbonate filter (pore size, 74 μm) at the bottom of a polystyrene upper chamber (Fig. 4*D*). At the indicated time of incubation, we counted the number of sperm that penetrated through the VE protein layer and infiltrated the lower chamber. The extent of penetration reached to maximum around 10 min (Fig. 4*F*). Pretreatment of VE with dicalcin (4 μM) significantly impaired the efficiency of sperm penetration 5 min after placement of sperm (~50% of control at 4 μM; $n = 6$, $p = 0.039$) (Fig. 4*G*).

Based on the above findings, we examined the effect of dicalcin on fertilization *in vitro*. Preincubation with anti-dicalcin antibody surprisingly increased the efficiency up to ~208% of control ($n = 6$, $p = 0.0074$) (Fig. 5*A*). Since anti-dicalcin antibody significantly blocked the binding of dicalcin to both gp41 and gp37 (Fig. 3*B*), preincubation with antibody is likely to neutralize the action of native dicalcin. Oppositely, preincubation with recombinant dicalcin inhibited the efficiency of fertilization in a dose-dependent manner (Fig. 5*B*). In particular, preincubation of dicalcin at a concentration of 4 μM inhibited fertilization almost completely (~14% of control; $n = 6$, $p = 7.2 \times 10^{-5}$). Addition of antibody (50 mg/liter) in the presence of 0.4 μM dicalcin cancelled this inhibitory action (+*Anti-dica* in Fig. 5*B*). Preincubation of EGTA (16 μM), equivalent to the amount of bound Ca^{2+} to dicalcin (4 μM), exerted no effect, which indicated that this inhibitory effect is not due to its Ca^{2+}-buffering ability but its action as a protein (*EGTA* in Fig. 5*B*). Preincubation of sperm with dicalcin (4 μM) had no effects, indicating that dicalcin acts on an egg, not on sperm (Fig. 5*C*). Taken together, these results strongly suggested that dicalcin dampens both of sperm binding and sperm penetration, and thereby reduces the efficiency of *in vitro* fertilization remarkably.

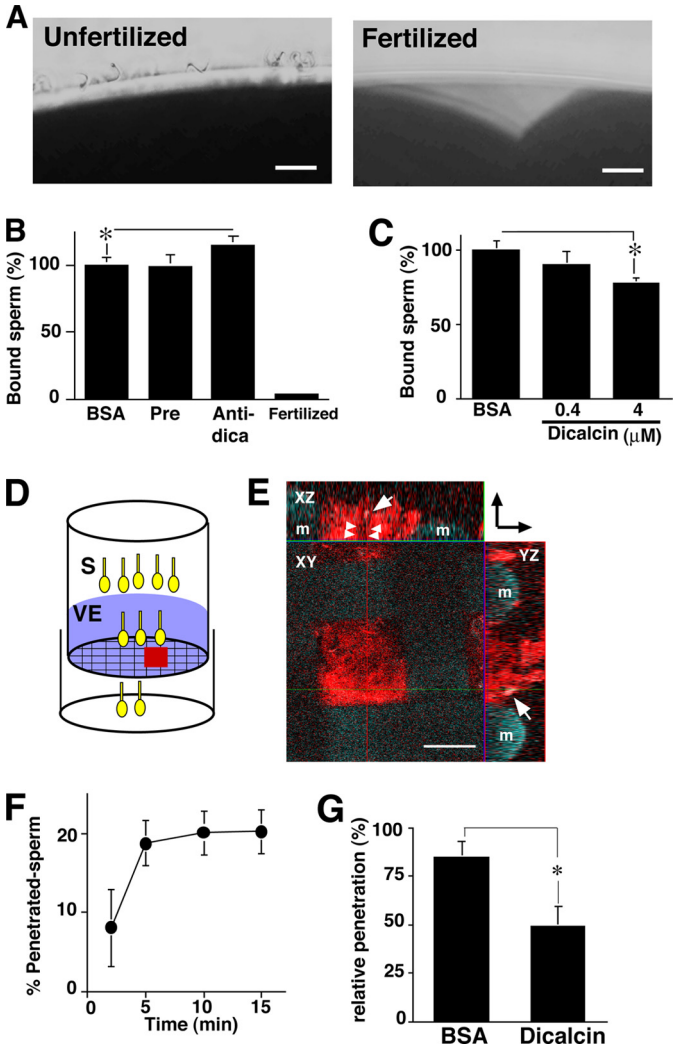

FIGURE 4. **Inhibitory effect of dicalcin on sperm binding and sperm penetration through the VE protein layer.** *A*, representative micrographs of unfertilized (*Unfertilized*) and fertilized (*Fertilized*) eggs after sperm treatment. *Scale bar*: 20 μm. *B*, effect of pretreatment with anti-dicalcin antibody on sperm binding to egg. Ovulated eggs were pretreated with preimmune antibody (*Pre*) or anti-dicalcin antibody (*Anti-dica*) followed by insemination. After rinse, bound sperm at an equatorial plane were counted ($n = 9$; *, $p = 0.027$). Almost no sperm remained attached to fertilized eggs (*Fertilized*). *C*, effect of pretreatment with dicalcin on sperm binding to egg. Ovulated eggs were pretreated with BSA or dicalcin at the indicated concentrations, and bound sperm were counted ($n = 9$; *, $p = 0.003$). *D*, a *scheme* that represents our *in vitro* penetration assay. Suspension of viscous VE proteins (*VE*) was placed on the mesh of the *upper chamber*. Some sperm (*S*) successfully penetrated through the VE. *E*, representative confocal image of Rhodamine-RCAI-treated VE proteins on the mesh of the *upper chamber* (*red square* in *D*). VE proteins stained with Rhodamine-RCAI (*red*) were observed. A penetrating spermatozoon stained with Hoechst 33342 was recognized in *XZ* and *YZ planes* (*arrows*). The potential trait of the spermatozoon through the VE is indicated (*arrowheads*). A direction from the *upper chamber* to the *lower one* is indicated (*arrows* at *upper right*). *m*, mesh. *Scale bar*: 50 μm. *F*, time course of sperm penetration. Sperm in the *lower chamber* were collected at the indicated times, and the percentage of the number of the penetrated sperm was calculated. The extent of penetration reached maximum at around 10 min. *G*, effect of pretreatment with dicalcin on sperm penetration. VE proteins on the *upper chamber* were pretreated either with dicalcin (4 μM) or BSA (4 μM) for 15 min, followed by sperm placement. After 5 min, sperm in the lower chamber were collected and the number of the penetrated sperm was calculated. The extent of penetration pretreated with BSA was set to ~100% ($n = 6$; *, $p = 0.039$). *BSA*, pretreated with BSA; *dicalcin*, pretreated with dicalcin.

Alteration of RCAI Reactivity of Vitelline Envelope Caused by Dicalcin—What is the molecular mechanism of an inhibitory effect of dicalcin on fertilization shown above? Carbohydrate-dependent recognition is well known to play an important role for establishment of an appropriate sperm-egg interaction. Accordingly, we hypothesized that dicalcin could induce an alteration in the interaction between sperm and VE glycans, thereby affecting the efficiency of fertilization. Interestingly, fertilization-failed human eggs showed a heterogeneous staining pattern by a lectin, *Maclura pomifera* that preferentially binds to terminal disaccharide galactose (Gal)-β1,3*N*-acetylgalactosamine (GalNAc) (29). In addition, another lectin, Wheat germ agglutinin, blocks fertilization *in vitro* in the hamster (30). Because Gal and GalNAc are presumed to be enriched in *Xenopus* VE glycans (23), Gal/GalNAc-sensitive lectin could detect some alterations in VE glycans (*e.g.* reactivity with lectin), which was caused by dicalcin. In addition, because removal of terminal sialic acid residues potentially unmasks Gal residues of glycoproteins in the mouse (31), sialic acid-sensitive lectin could also be used to detect an alteration of VE glycans. Therefore, we examined the reactivity of VE glycoproteins with Gal/GalNAc-sensitive lectins, RCAI, soybean agglutinin, as well as sialic acid-sensitive lectins, *S. nigra* lectin and *Maackia amurensis* lectin II. Among them, neither soybean agglutinin, *S. nigra* lectin, or *M. amurensis* lectin II showed reactivities, while RCAI solely reacted with gp41, one of the targets of dicalcin, in our lectin blot analysis (Fig. 6*A*). This reactivity disappeared when RCAI was preabsorbed with VE proteins (not shown). When RCAI-staining signals were quantified across the VE by line scan analyses, pretreatment of dicalcin increased the peak RCAI signal to ~120% of control in the outermost region of VE (Fig. 6*C*). Furthermore, when the signal was detected under higher gain, surprisingly, it was revealed that pretreatment of dicalcin significantly broadened the RCAI-reactive zone (Fig. 6*D*) and disclosed the clear RCAI signal at the interface between VE and egg plasma membrane (*arrows*, Fig. 6, *B* and *D*). Because RCAI reacted neither with BSA nor dicalcin (Fig. 6*E*), these results indicated that pretreatment of dicalcin increases RCAI reactivity of gp41 in the VE.

Mechanisms Underlying Dicalcin-dependent Regulation of Distribution of Oligosaccharides in the Vitelline Envelope—How is the above alteration in RCAI reactivity brought about by exogenous dicalcin? We hypothesized two models: one is the "glycoprotein" model and the other is the "VE structure" model, although these two models are not mutually exclusive. In our glycoprotein model, dicalcin binds to gp41 and induces allosteric conformational change of gp41 molecule, increasing its RCAI reactivity. In our VE structure model, dicalcin binds to gp41 as well as gp37 and induces changes in the three-dimensional structure of filamentous network of VE (32), increasing the accessibility of macromolecules such as RCAI within the VE. To verify the first scenario, we examined the increased binding ability of gp41 to RCAI by blot overlay and FCS analyses. In blot overlay analysis, blots of VE proteins were preincubated either in the presence or absence of dicalcin and Ca^{2+}, followed by incubation of RCAI. The amount of bound RCAI was significantly

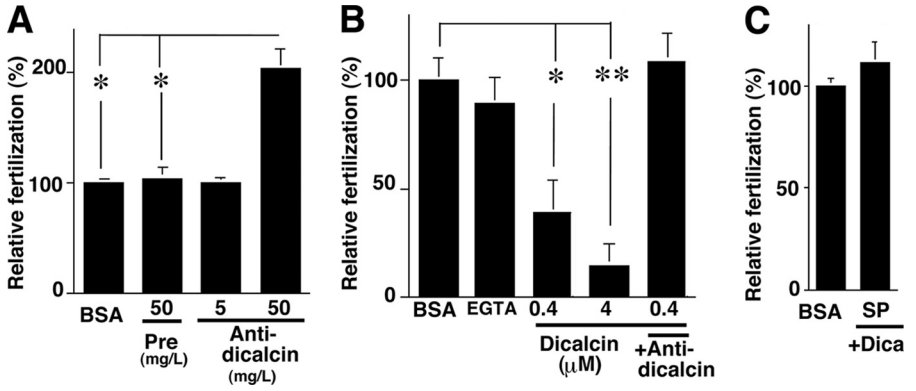

FIGURE 5. **Inhibitory effect of dicalcin on *in vitro* fertilization.** *A*, effect of pretreatment with anti-dicalcin antibody on fertilization. Ovulated eggs were pretreated with preimmune antibody (*Pre*, 50 mg/liter) or anti-dicalcin (*Anti-dica*, 5 and 50 mg/liter) followed by incubation of sperm. The number of two-cell embryos was counted until one of the embryos proceeded to the four-cell-stage. Fertilization success was scored and normalized ($n = 6$; *, $p = 0.007$). *B*, effect of pretreatment with dicalcin on fertilization. Ovulated eggs were pretreated with BSA or dicalcin at indicated concentrations followed by insemination ($n = 6$; *, $p = 0.004$; **, $p = 7.2 \times 10^{-5}$). *EGTA*: addition of EGTA (16 μM) prior to inseminations. +*Anti-dica*: addition of anti-dicalcin antibody (50 mg/liter) together with dicalcin. *C*, effect of preincubation of sperm with dicalcin on fertilization. Ovulated eggs were inseminated with sperm (*SP*) that were preincubated with dicalcin (*Dica*). As a control, eggs were pretreated with BSA (*BSA*) similarly as described above and inseminated with sperm.

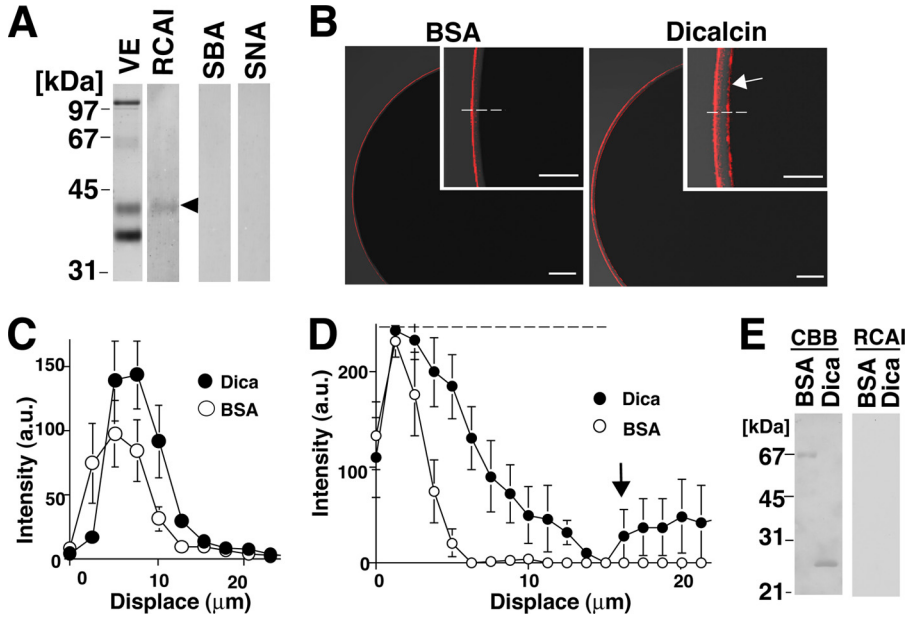

FIGURE 6. **Dicalcin induced increases in RCAI reactivity of vitelline envelope.** *A*, blots of vitelline envelope (*VE*) were treated with one of fluorescently labeled lectins (RCAI, soybean agglutinin (*SBA*), or *S. nigra* (*SNA*). RCAI recognized gp41 (*arrowhead*). *B*, representative confocal images of a *Xenopus* egg treated with RCAI. Unfertilized eggs were preincubated either with BSA or dicalcin, followed by RCAI staining. *Insets*: higher magnified images. RCAI signal at the interface between VE and egg plasma membrane is indicated (*arrow*). *Scale bar*: 50 μm. *C*, averaged line scans of RCAI staining across the VE under lower sensitive detection. Intensities of RCAI staining were profiled across the VE (*dashed line* in *B*) either in the preincubation of BSA (*BSA*) or dicalcin (*Dica*) ($n = 7$). The position where RCAI signal starts to rise is designated as 0 μm in the *x* axis. *D*, averaged line scans of RCAI staining across the VE under higher sensitive detection. Intensities of RCAI staining were profiled as stated in *C* ($n = 7$). The *dashed line* shows the saturating level of the intensity detection. An increase in RCAI signal at the interface between VE and egg plasma membrane is indicated (*arrow*). *E*, neither BSA nor dicalcin reacted with RCAI. *CBB*, CBB-staining of BSA and dicalcin after SDS-PAGE; *RCAI*, RCAI blot.

increased in the presence of dicalcin (4 μM) and Ca^{2+} (200 μM) (Fig. 7*A*, *middle*; ~163% of control, $n = 8$, $p = 0.002$). To further confirm this increase, we performed FCS measurement, where the diffusion of fluorescence in a small defined confocal volume is recorded as fluctuated fluorescence intensity (Fig. 7*C*). Subsequent autocorrelation analyses of these fluctuations estimate diffusion time of fluorescent molecules and distinguish small fast diffusing (*i.e.* free fluorescent molecules) and large slow moving (target-bound molecules), which enabled us to investigate the stoichiometry of binding (for reviews see Refs. 33, 34). Isolated gp41 was coupled with the fluorescent dye, TMR. By addition of RCAI, diffusion time of TMR-labeled gp41 increased, which confirmed the binding of TMR-gp41 to RCAI (data not shown). Fitting the binding data with a Hill equation revealed significant alteration in apparent K_d values: ~0.3 and ~1.5 μM in the presence and absence of dicalcin, respectively (Fig. 7*D*). Accordingly, both solid-phase (blot overlay analysis) and liquid-phase (FCS analysis) analyses indicate that the dicalcin-bound gp41 has a more ability to bind to RCAI, which supports our glycoprotein model. Next, to verify the VE structure model, we quantitatively assessed dicalcin-dependent structural change in the VE by *in vivo* labeling with fluorescent dye (Fig. 8*A*). Extracellularly applied fluorescent dye, Cy5, successfully labeled each of the VE proteins (supplemental Fig. S1). This commercially prepared dye is validated to couple one molecule of Cy5 with one molecule of protein at a low dye-to-protein ratio (<1%, see manufacturer's manual), and therefore the amount of fluorescence virtually reflects the number of labeled protein. Preincubation of VE with dicalcin (4 μM) resulted in significantly greater Cy5 incorporation in each of four major VE proteins compared with control (Fig. 8*B*). The calculated ratio of labeled protein to VE-existed protein increased to approximately twice that of control (180–240% of control, $n = 8$–10, $p = 0.002$–0.02) (Fig. 8*C*). Intriguingly, these increases occurred in every VE protein, not solely in gp37 or gp41, which indicates that dicalcin binding to gp37 and gp41 caused changes in the three-dimensional structure of the entire VE framework, allowing every VE protein to be more accessible to the solvent. Additionally, this change may also involve geometrical arrangement of gp41 where gp41 molecules reside in the close proximity and form the clusters of their glycans. Because a lectin generally exhibits a high affinity with gly-

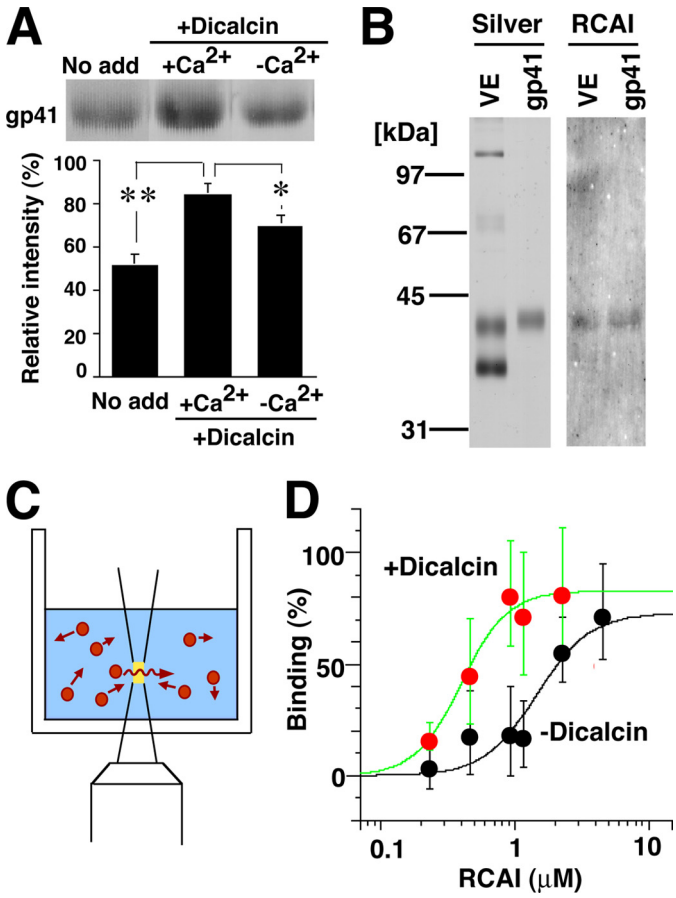

FIGURE 7. **Dicalcin binding to gp41 increases the reactivity of gp41 with RCAI.** *A*, blots of VE proteins were preincubated in the presence or absence of dicalcin and Ca^{2+}, followed by incubation with Rhodamine-labeled RCAI. Representative RCAI binding to gp41 was indicated (*upper*). The normalized intensity was significantly increased in the presence of dicalcin and Ca^{2+} (*lower graph*, $n = 8$; *, $p = 0.06$; **, $p = 0.002$). *No add*, nothing preincubated; *+Dicacin*, preincubation with dicalcin (1 μM); $+Ca^{2+}$, preincubation in the presence of Ca^{2+} (500 μM $CaCl_2$); $-Ca^{2+}$, preincubation in the absence of Ca^{2+} (500 μM EGTA). *B*, isolation of gp41. *Silver*, silver-stained VE proteins and isolated gp41; *RCAI*, blot with RCAI. *C*, a *scheme* that represents FCS measurement. A fluorescent signal of diffusing molecule (*red*) was detected within a small defined confocal volume (*yellow*) of the well. Autocorrelation analyses of the fluctuating fluorescent signal estimate the diffusion time of fluorescent molecules and distinguish small fast diffusing (*i.e.* free fluorescent molecules) and large slow moving (target-bound molecules); this enabled us to investigate the stoichiometry of binding. *D*, the binding of TMR-labeled gp41 to RCAI was analyzed with FCS either in the presence of 1 μM dicalcin (*red circles*) or absence of dicalcin (*black circles*) ($n = 15$). Maximum and minimum diffusion time in each measurement was set to 100 and 0% binding, respectively. Each group of data were fitted with a Hill equation.

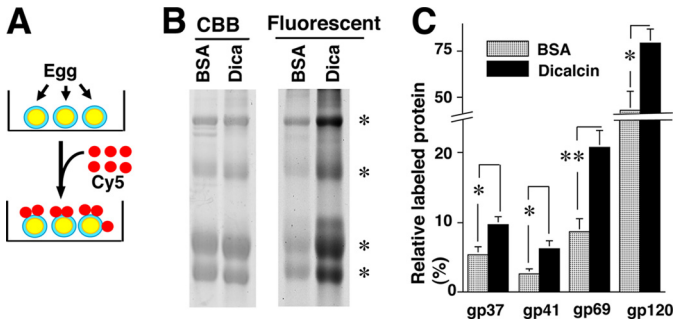

FIGURE 8. **Dicalcin binding to gp41 increases exposure of gp41 to an external environment.** *A*, a *scheme* that represents *in vivo* labeling of the VE with fluorescent dye, Cy5. Dejellied eggs were labeled with exogenously applied Cy5 in 0.3×MMR. *B*, after preincubation either with BSA (*BSA*) or dicalcin (*Dica*), labeled VE proteins were electrophoresed and fluorescent image was obtained, followed by CBB staining to quantitate the amount of each VE protein (*asterisks*). *CBB*, CBB staining of VE proteins; *Fluorescent*, fluorescent image of Cy5-labeled VE proteins. *BSA*, preincubated with BSA; *Dica*, preincubated with dicalcin. *C*, the ratio of the molar amount of labeled protein to the total amount existing in the preparation was calculated for each VE protein. The highest ratio for gp120, when preincubated with dicalcin, was set to 100% in each trial, and data were normalized. *BSA*, preincubated with BSA; *Dicalcin*, preincubated with dicalcin ($n = 8–10$; *, $p < 0.02$; **, $p = 0.002$).

cans in clusters, this arrangement could account for a dicalcin-dependent increase in RCAI reactivity of VE. We discuss the possible molecular details regarding the action of dicalcin below.

DISCUSSION

In our present study, we found that dicalcin is localized prominently in the *Xenopus* VE, an extracellular matrix that surrounds an egg, as well as intracellular cytoplasm in the cortex region of an egg (Fig. 2*C*). In the VE, dicalcin binds to protein cores of gp41 and gp37, constituents of the filamentous network of the VE (Fig. 3), raising the interesting possibility that dicalcin affects the fertilization processes. Actually, dicalcin dampens both sperm binding and sperm penetration, exerting a crucial role in the regulation of the fertilization (Figs. 4 and 5).

Several treatments have been known to affect fertilization. Exogenous application of VE proteins interfered with the sperm-egg binding, and several glycosidase treatments of VE proteins reduced the binding ability to sperm (8, 28). Compared with these inhibitory treatments, however, there have been few treatments to increase the efficiency of fertilization. The only exception is sialidase treatment of the mouse egg that increases the efficiency up to ~130% of control (31). Our present study demonstrated a unique action of dicalcin on fertilization: almost complete inhibition (~15% of control) in its gain-of-function state, whereas remarkable increase (~208% of control) in its loss-of-function state (Fig. 5). Therefore, it seems likely that dicalcin, as an extracellular mediator of fertilization, is capable of controlling either favorable or unfavorable conditions for sperm-egg interaction in *X. laevis*.

Fertilization processes are considered to involve oligosaccharide-mediated events, although the exact mechanism remains elusive. We discovered that dicalcin alters the distribution of oligosaccharides within the VE, correlating its suppressive action on fertilization (Fig. 6). This alteration is possibly a consequence of two mutually compatible mechanisms: one is brought about by the increase in binding ability of gp41 to RCAI (Fig. 7, *A* and *D*, referred to as the glycoprotein model), and the other is the structural change of the entire VE (Fig. 8*C*, referred to as the VE structure model). We tentatively propose molecular details of both models (for schematic models, see Fig. 9). In our glycoprotein model, the Ca^{2+}-bound form of dicalcin binds to gp41 and induces a conformational change, which causes an exposure of RCAI ligands. This allosteric change in the configuration of oligosaccharides may mask sperm receptors, forming a functional "barrier" to prevent sperm binding (Fig. 9*A*), which may underlie a dicalcin-dependent

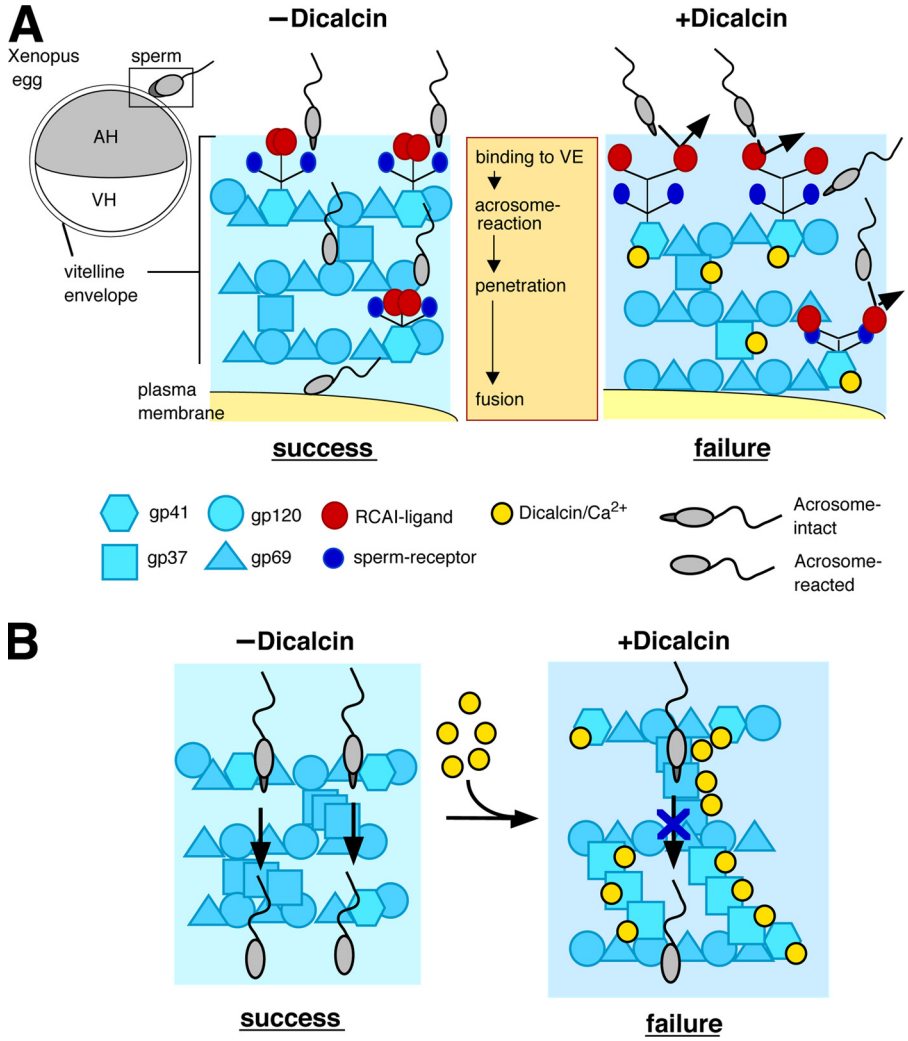

FIGURE 9. **Schematic models of the inhibitory action of dicalcin on fertilization in *X. laevis*.** *A*, glycoprotein model that involves allosteric conformational change of gp41 caused by dicalcin. In a currently favored model in *Xenopus* egg, acrosome-intact sperm bind to gp41 (a frog orthologue of mouse ZP3; a major binding partner of sperm) and gp69/64 (an orthologue of mouse ZP2) via carbohydrate moieties (sperm receptors). After acrosome reaction, sperm penetrate through the VE and fuse with an egg (*−Dicalcin*). The Ca^{2+}-bound form of dicalcin binds to gp41 (and gp37 additionally), leading to a conformational change that could cause an exposure of RCAI ligands. This allosteric change in the configuration of oligosaccharides may mask sperm receptors, forming a functional barrier to prevent sperm binding, penetration, and fusion (*+Dicalcin*). *AH*, animal hemisphere; *VH*, vegetal hemisphere. *B*, VE structure model that involves structural change in the VE framework caused by dicalcin. VE proteins (gp37, gp41, gp69/64, and gp120) associate with each other and constitute the filament of VE (depicted in *−Dicalcin*; modified from the schematic model in mammalian ZP). Dicalcin binding to gp37 and gp41 caused a structural change in the three-dimensional structure of the filamentous VE network. This change may involve disorganization of filaments, including fasciculation of filaments, and cause enlargement of the pore size among VE filaments as depicted in *+Dicalcin*. *Symbols* are the same in *A* and *B*.

slight reduction in sperm binding (~20% decrease of control (Fig. 4*C*)). On the other hand, in our VE structure model, dicalcin binding to gp37 and gp41 caused the three-dimensional structural change in the filamentous VE network, which might dampen the proper interaction between sperm and VE and prevent the induction of sperm acrosome reaction (Fig. 9*B*). This may account for substantial reductions both in sperm penetration (~50% decrease compared with control (Fig. 4*G*)) and subsequent *in vitro* fertilization (~85% decrease (Fig. 5*B*)) in the presence of exogenous dicalcin.

Several lines of evidence from biochemical experiments have implicated some terminal residues of the glycans of envelope-constituent glycoprotein (*e.g.* Galα1–3Gal sequence and/or β-linked GlcNAc) as essential carbohydrates for sperm recognition. However, later gene-disruption studies and mass spectrometry analyses using a native egg-coating envelope do not support a model in which sperm binding to the egg-coating envelope is dependent on a particular glycan of the glycoprotein (5). Instead, attention has been drawn to a particular three-dimensional structure of the egg-coating envelope that makes the structure susceptible for sperm binding (3). As a macrostructure, the thickness of human zona pellucida correlates with the fertilization rate in human (35). On a more detailed scale, the appropriate pore size of VE filament is thought to be important for generating shear force-dependent mechanosensory signaling and a subsequent acrosome reaction (36). These lines of evidence suggested that the proper organization of the egg-coating membrane is relevant to the success of fertilization. In accordance with this, our results imply that the three-dimensional distribution of oligosaccharides within the VE is important for an appropriate sperm-egg interaction. It is of interest to determine whether dicalcin-dependent changes in the entire VE structure may involve disorganization of filaments, including fasciculation of filaments and/or enlargement of pore size among VE filaments.

In conclusion, we identified *Xenopus* dicalcin in the extracellular egg-coating envelope. Dicalcin binds to an envelope-constituent glycoprotein and alters the configuration of oligosaccharide portions of them, affecting the distribution of oligosaccharides within the envelope. Correlating with this alteration, dicalcin regulates both sperm binding and sperm penetration processes and thereby plays a suppressive role in the sperm-egg interaction during fertilization. We believe that our present study would provide insights to define highly coordinated molecular mechanisms of fertilization.

Acknowledgment—We thank T. Uebi at Osaka University for comments and technical assistance.

REFERENCES

1. Yanagimachi, R. (1994) in *The Physiology of Reproduction* (Knobil, E., and Neill, J. D., eds) pp. 189–317, Raven Press, New York
2. Primakoff, P., and Myles D. G. (2002) *Science* **296,** 2183–2185
3. Hoodbhoy, T., and Dean, J. (2004) *Reproduction* **127,** 417–422
4. Litscher, E. S., and Wassarman, P. M. (2007) *Histol. Histopathol.* **22,** 337–347
5. Clark, G. F., and Dell, A. (2006) *J. Biol. Chem.* **281,** 13853–13856
6. Miller, D. J., Macek, M. B., and Shur, B. D. (1992) *Nature* **357,** 589–593
7. Bookbinder, L. H., Cheng, A., and Bleil, J. D. (1995) *Science* **269,** 86–89
8. Vo, L. H., and Hedrick, J. L. (2000) *Biol. Reprod.* **62,** 766–774
9. Bork, P., and Sander, C. (1992) *FEBS Lett.* **300,** 237–240
10. Kubo, H., Kawano, T., Tsubuki, S., Kawashima, S., Katagiri, C., and Suzuki, A. (1997) *Dev. Growth Differ.* **39,** 405–417
11. Vo, L. H., Yen, T. Y., Macher, B. A., and Hedrick, J. L. (2003) *Biol. Reprod.* **69,** 1822–1830
12. Miwa, N., Shinmyo, Y., and Kawamura, S. (2007) *DNA Seq.* **18,** 400–404
13. Heizmann, C. W., Fritz, G., and Schäfer, B. W. (2002) *Front. Biosci.* **7,** 1356–1368
14. Donato, R. (2003) *Microsc. Res. Tech.* **60,** 540–551
15. Miwa, N., Kobayashi, M., Takamatsu, K., and Kawamura, S. (1998) *Biochem. Biophys. Res. Commun.* **251,** 860–867
16. Miwa, N., Uebi, T., and Kawamura, S. (2000) *J. Biol. Chem.* **275,** 27245–27249
17. Uebi, T., Miwa, N., and Kawamura, S. (2007) *FEBS J.* ***274,*** 4863–4876
18. Miwa, N., Shinmyo, Y., and Kawamura, S. (2001) *Eur. J. Biochem.* **268,** 6029–6036
19. David, G., Barrett, J. N., and Barrett, E. F. (1997) *J. Physiol.* **504,** 83–96
20. Wolf, D. P., Nishihara, T., West, D. M., Wyrick, R. E., and Hedrick, J. L. (1976) *Biochemistry* **15,** 3671–3678
21. Richter, H. P. (1980) *Cell Biol. Int. Rep.* **4,** 985–995
22. Lindsay, L. L., and Hedrick, J. L. (1988) *J. Exp. Zool.* **245,** 286–293
23. Lindsay, L. L., and Hedrick, J. L. (1989) *Dev. Biol.* **135,** 202–211
24. Heasman, J., Holwill, S., and Wylie, C. C. (1991) *Methods Cell Biol.* **36,** 213–230
25. Ihara, S., Miyoshi, E., Ko, J. H., Murata, K., Nakahara, S., Honke, K., Dickson, R. B., Lin, C. Y., and Taniguchi, N. (2002) *J. Biol. Chem.* **277,** 16960–16967
26. Rammes, A., Roth, J., Goebeler, M., Klempt, M., Hartmann, M., and Sorg, C. (1997) *J. Biol. Chem.* **272,** 9496–9502
27. Davey, G. E., Murmann, P., and Heizmann, C. W. (2001) *J. Biol. Chem.* **276,** 30819–30826
28. Tian, J., Gong, H., Thomsen, G. H., and Lennarz, W. J. (1997) *J. Cell Biol.* **136,** 1099–1108
29. Talevi, R., Gualtieri, R., Tartaglione, G., and Fortunato, A. (1997) *Hum. Reprod.* **12,** 2773–2780
30. Oikawa, T., Yanagimachi, R., and Nicolson G. L. (1973) *Nature* **241,** 256–259
31. Mori, E., Mori, T., and Takasaki, S. (1997) *Biochem. Biophys. Res. Commun.* **238,** 95–99
32. Larabell, C. A., and Chandler, D. E. (1988) *Cell Tissue Res.* **251,** 129–136
33. Pramanik, A., and Rigler, R. (2001) in *Fluorescence Correlation* Spectroscopy (Elson, E., and Rigler, R., eds) pp. 101–129, Springer, Heidelberg, Germany
34. Medina, M. A., and Schwille, P. (2002) *BioEssays* **24,** 758–764
35. Bertland, E., Van den Bergh, M., and Englert, Y. (1995) *Hum. Reprod.* **10,** 1189–1193
36. Baibakov, B., Gauthier, L., Talbot, P., Rankin, T. L., and Dean, J. (2007) *Development* **134,** 933–943